



375-nm ultraviolet-laser based non-line-of-sight underwater optical communication

XIAOBIN SUN,¹ WENQI CAI,¹ OMAR ALKHAZRAGI,^{1,2} EE-NING OOI,¹
HONGSEN HE,¹ ANAS CHAABAN,^{1,4} CHAO SHEN,¹ HASSAN MAKINE OUBEI,¹
MOHAMMED ZAHED MUSTAFA KHAN,² TIEN KHEE NG,¹ MOHAMED-SLIM
ALOUINI,^{3,5} AND BOON S. OOI^{1,6}

¹Photonics Laboratory, King Abdullah University of Science & Technology (KAUST), Thuwal 23955-6900, Saudi Arabia

²Optoelectronics Research Laboratory, Electrical Engineering Department, King Fahd University of Petroleum and Minerals (KFUPM), Dhahran 31261, Saudi Arabia

³Communication Theory Laboratory, King Abdullah University of Science & Technology (KAUST), Thuwal 23955-6900, Saudi Arabia

⁴Currently in School of Engineering, the University of British Columbia, Kelowna, BC V1Y 1V7, Canada

⁵slim.alouini@kaust.edu.sa

⁶boon.ooi@kaust.edu.sa

Abstract: For circumventing the alignment requirement of line-of-sight (LOS) underwater wireless optical communication (UWOC), we demonstrated a non-line-of-sight (NLOS) UWOC link adequately enhanced using ultraviolet (UV) 375-nm laser. Path loss was chosen as a figure-of-merit for link performance in this investigation, which considers the effects of geometries, water turbidity, and transmission wavelength. The experiments suggest that path loss decreases with smaller azimuth angles, higher water turbidity, and shorter wavelength due in part to enhanced scattering utilizing 375-nm radiation. We highlighted that it is feasible to extend the current findings for long distance NLOS UWOC link in turbid water, such as harbor water.

© 2018 Optical Society of America under the terms of the [OSA Open Access Publishing Agreement](#)

OCIS codes: (260.7190) Ultraviolet; (010.4458) Oceanic scattering; (010.7340) Water; (140.3460) Lasers.

References and links

1. Z. Zeng, S. Fu, H. Zhang, Y. Dong, and J. Cheng, "A Survey of Underwater Optical Wireless Communications," *IEEE Comm. Surv. and Tutor.* **19**(1), 204–238 (2017).
2. M. A. Khalighi and M. Uysal, "Survey on free space optical communication: A communication theory perspective," *IEEE Comm. Surv. and Tutor.* **16**(4), 2231–2258 (2014).
3. C. Mobley, *Light and Water: Radiative Transfer in Natural Waters* (Academic, 1994).
4. M. Chitre, S. Shahabudeen, L. Freitag, and M. Stojanovic, "Recent advances in underwater acoustic communications networking," in *Proceedings of IEEE Conference on Oceans* (IEEE, 2008), pp. 1–10.
5. R. E. Williams and H. F. Battestin, "Coherent Recombination of Acoustic Multipath Signals Propagated in the Deep Ocean," *J. Acoust. Soc. Am.* **50**(6A), 1433–1442 (1971).
6. C. Xilin, Q. Fengzhong, and Y. Liuqing, "Single carrier fdma over underwater acoustic channels," in *Proceedings of IEEE Conference on Communications and Networking* (IEEE, 2011), pp. 1052–1057.
7. B. Li, S. Zhou, M. Stojanovic, L. Freitag, and P. Willett, "Multicarrier Communication Over Underwater Acoustic Channels With Nonuniform Doppler Shifts," *IEEE J. Oceanic Eng.* **33**(2), 198–209 (2008).
8. X. Liu, S. Yi, X. Zhou, Z. Fang, Z.-J. Qiu, L. Hu, C. Cong, L. Zheng, R. Liu, and P. Tian, "34.5 m underwater optical wireless communication with 2.70 Gbps data rate based on a green laser diode with NRZ-OOK modulation," *Opt. Express* **25**(22), 27937–27947 (2017).
9. C. Shen, Y. Guo, H. M. Oubei, T. K. Ng, G. Liu, K.-H. Park, K.-T. Ho, M.-S. Alouini, and B. S. Ooi, "20-meter underwater wireless optical communication link with 1.5 Gbps data rate," *Opt. Express* **24**(22), 25502–25509 (2016).
10. Y. Chen, M. Kong, T. Ali, J. Wang, R. Sarwar, J. Han, C. Guo, B. Sun, N. Deng, and J. Xu, "26 m/5.5 Gbps air-water optical wireless communication based on an OFDM-modulated 520-nm laser diode," *Opt. Express* **25**(13), 14760–14765 (2017).

11. J. J. D. McKendry, R. P. Green, A. E. Kelly, Z. Gong, B. Guilhabert, D. Massoubre, E. Gu, and M. D. Dawson, "High-Speed Visible Light Communications Using Individual Pixels in a Micro Light-Emitting Diode Array," *IEEE Photonics Technol. Lett.* **22**(18), 1346–1348 (2010).
12. J. Xu, Y. Song, X. Yu, A. Lin, M. Kong, J. Han, and N. Deng, "Underwater wireless transmission of high-speed QAM-OFDM signals using a compact red-light laser," *Opt. Express* **24**(8), 8097–8109 (2016).
13. A. Al-Halafi, H. M. Oubei, B. S. Ooi, and B. Shihada, "Real-time video transmission over different underwater wireless optical channels using a directly modulated 520 nm laser diode," *IEEE/OSA, J. Opt. Commun. Netw.* **9**(10), 826–832 (2017).
14. G. L. Harvey, "A survey of ultraviolet communication systems," Naval Research Laboratory Technical Report, Washington D.C., March 1964.
15. D. E. Sunstein, "A scatter communications link at ultraviolet frequencies," B.S. Thesis, MIT, Cambridge, MA, 1968.
16. S. Tang, Y. Dong, and X. Zhang, "On path loss of nlos underwater wireless optical communication links," in *Proceedings of IEEE Conference on Oceans* (IEEE, 2013), pp. 1–3.
17. W. Liu, D. Zou, Z. Xu, and J. Yu, "Non-line-of-sight scattering channel modeling for underwater optical wireless communication," in *IEEE International Conference on Cyber Technology in Automation, Control, and Intelligent Systems* (IEEE, 2015), pp. 1265–1268.
18. D. Alley, L. Mullen, and A. Laux, "Compact, dual-wavelength, non-line-of-sight (nlos) underwater imager," in *Proceedings of IEEE Conference on Oceans* (IEEE, 2011), pp. 1–5.
19. C. Gabriel, M. A. Khalighi, S. Bourennane, P. Leon, and V. Rigaud, "Monte-Carlo-based channel characterization for underwater optical communication systems," *IEEE/OSA J. Opt. Commun. Netw.* **5**(1), 1–12 (2013).
20. A. Choudhary, F. M. Bui, and P. Muthuchidambaranathan, "Characterization of channel impulse responses for nlos underwater wireless optical communications," in *Proceedings of IEEE Conference on Advances in Computing and Communications* (IEEE, 2014), pp. 77–79.
21. V. K. Jagadeesh, K. V. Naveen, and P. Muthuchidambaranathan, "BER Performance of NLOS Underwater Wireless Optical Communication with Multiple Scattering," *Int. J. Res. Schol. Innov.* **9**(2), 562–566 (2015).
22. K. J. V., A. Choudhary, V. K. Jagadeesh, and P. Muthuchidambaranathan, "Pathloss analysis of nlos underwater wireless optical communication channel," in *Proceedings of IEEE Conference on Oceans on Electronics and Communication Systems* (IEEE, 2014), pp. 1–4.
23. S. Q. Duntley, "Light in the Sea," *J. Opt. Soc. Am. A* **53**(2), 214–233 (1963).
24. H. M. Oubei, C. Li, K.-H. Park, T. K. Ng, M.-S. Alouini, and B. S. Ooi, "2.3 Gbit/s underwater wireless optical communications using directly modulated 520 nm laser diode," *Opt. Express* **23**(16), 20743–20748 (2015).
25. H. M. Oubei, J. R. Duran, B. Janjua, H.-Y. Wang, C.-T. Tsai, Y.-C. Chi, T. K. Ng, H.-C. Kuo, J.-H. He, M.-S. Alouini, G.-R. Lin, and B. S. Ooi, "4.8 Gbit/s 16-QAM-OFDM transmission based on compact 450-nm laser for underwater wireless optical communication," *Opt. Express* **23**(18), 23302–23309 (2015).
26. M. Jonasz, G. Fournier, and I. ebrary, *Light Scattering by Particles in Water: Theoretical and Experimental Foundations* (Academic, 2007).
27. A. Laux, R. Billmers, L. Mullen, B. Concannon, J. Davis, J. Prentice, and V. Contarino, "The a, b, cs of oceanographic lidar predictions: a significant step toward closing the loop between theory and experiment," *J. Mod. Opt.* **49**(3-4), 439–451 (2002).
28. T. J. Petzold, "Volume Scattering Functions for Selected Ocean Waters," Visibility Laboratory Tech. Report 72–78, Scripps Institution of Oceanography, San Diego, Calif. (1972).
29. B. M. Cochenour, L. J. Mullen, and A. E. Laux, "Characterization of the Beam-Spread Function for Underwater Wireless Optical Communications Links," *IEEE J. Oceanic Eng.* **33**(4), 513–521 (2008).
30. W. Cox and J. Muth, "Simulating channel losses in an underwater optical communication system," *J. Opt. Soc. Am. A* **31**(5), 920–934 (2014).
31. H. M. Oubei, R. T. ElAfandy, K. H. Park, T. K. Ng, M. S. Alouini, and B. S. Ooi, "Performance Evaluation of Underwater Wireless Optical Communications Links in the Presence of Different Air Bubble Populations," *IEEE Photonics J.* **9**(2), 1–9 (2017).
32. M. Lanzagorta, *Underwater communications* (Morgan & Claypool, 2012).
33. R. C. Smith and K. S. Baker, "Optical properties of the clearest natural waters (200-800 nm)," *Appl. Opt.* **20**(2), 177–184 (1981).
34. N. G. Jerlov, *Marine Optics* (Elsevier, 1976).
35. B. Cochenour and L. Mullen, "Free-space optical communications underwater" in *Advanced Optical Wireless Communication Systems*, J. B. S. Arnon, G. Karagiannidis, R. Schober, and M. Uysal, ed. (Cambridge University, 2012), pp. 201–239.
36. N. B. Divari, *The Height of the Twilight Ray* (Springer, 1970).

1. Introduction

Underwater wireless communication (UWC) is of great interest to the military, industry, and the scientific communities due to various applications ranging from tactical surveillance, pipeline and environmental monitoring to oceanographic data survey, marine archaeology, and search or research missions [1,2]. Yet the radio frequency (RF) communication system

widely utilized for the terrestrial communication can hardly be deployed underwater due to high seawater attenuation [3]. Acoustic communication is the commercially viable solution so far, due to the long propagation distance over kilometers in the water [4,5], but it is limited in data-rate by the low channel bandwidth underwater and the high latency [6,7].

Given these inherent drawbacks in RF and acoustic channels, underwater wireless optical communications (UWOC) turns out to be an appropriate solution for real-time high-data-rate communication at giga-bits-per-second over 20 meters [8–10]. Moreover, in the industry, the underwater transmission distance has been extended over 150 m with a data rate of 12.5 Mbps, as demonstrated by Sonardyne's BlueComm 200 system. Furthermore, the advancements of low-cost and energy-efficient light sources such as LEDs [11] and diode lasers [12] enable the construction of compact miniaturized optical transceivers for data, image, and video transmission [13].

The aforementioned works mainly consider line-of-sight (LOS) configuration, which inherently imposes strict requirements on positioning, acquisition, and tracking (PAT) [14,15]. In underwater conditions, the transmitted photons are scattered and absorbed by water molecules, dissolved ions, organic matters, and suspended particulates or planktonic organisms. Underwater LOS communication link may also be obstructed by hills and rocks. Both of these scenarios will lead to scintillation, deep-fading, or complete loss of signals. To this end, non-line-of-sight (NLOS) communication can be implemented to mitigate the abovementioned issues, which can be implemented either through light reflection from the water surface [16] or light scattering [17] from the molecules in the water. A diffused-reflection NLOS communication can also be implemented; for example in [18], which reported a 500 kbps, 6.6 m link.

Path loss can be adopted as a figure-of-merit to study NLOS communication channel as lower path loss indicates higher communication data rate and received signal-to-noise ratio (SNR) performances. It is affected not only by the channel geometries but also the water turbidity, transmission power, and wavelength utilized in the data transmission channel. It is noted that in the literature merely reports on simulation works, for instance those based on Monte Carlo method [19] and Henyey-Greenstein (HG) phase function [3], including impulse response [17,20], bit-error rate (BER) performance predictions [17,21] as well as the effect of channel geometries on path loss [22]. Experimental data is much needed to guide the experimental design of eventual long-distance NLOS transmission.

In this paper, we demonstrate the merits of NLOS UWOC link based on 375-nm laser in which link performance can be enhanced predominantly through multiple scattering. For a comprehensive evaluation, we experimentally measured the effect of geometries, water turbidity, and wavelengths on path-loss. On the significance of the present work, we noted that previous wavelength used in UWOC are mainly in the "transparent window" (400~600 nm) for light aquatic-attenuation [23–25]. However, to achieve both low light aquatic attenuation and high scattering for achieving a good NLOS UWOC link, we use the enhanced scattering property of 375 nm. To the best of our knowledge, this is the first experimental investigation of NLOS UWOC based on 375-nm diode laser.

2. Experiment details

The experimental setup is depicted in Fig. 1. The transmitter consisted of an ultraviolet diode laser (Thorlabs L375P70MLD) with a maximum output power of 70 mW and a peak wavelength of 375 nm. For cooling and heat-sinking, the laser is mounted on Thorlabs TCLDM9, which is connected to Thorlabs ITC4001 laser-diode and thermoelectric cooler (TEC) controller. Meanwhile, to demonstrate the significant advantage of 375-nm, the path loss data was compared to a 405-nm diode-pumped solid-state (DPSS) laser (Changchun New Industries MDL-III-405-500mW) with a maximum output power of 500 mW and a peak wavelength of 405 nm, whose wavelength is in the "transparent window". A series of plano-convex lenses are used for collimating the laser beam.

The laser beam propagates through the transparent glass water tank, which has a transmittance of $\sim 94\%$ at the wavelengths under investigation. Φ_{Tx} in Fig. 1 is the beam divergence angle, which changes in various water conditions due to different scattering effects. φ_{Tx} is the transmitter azimuth angle that can be changed using a rotation stage. Besides, the transmitter and receiver are placed in a coplanar configuration.

A water tank with dimensions of length 45 cm \times width 30 cm \times height 35 cm is utilized. Except for the incident glass wall (45cm \times 35 cm), the other inner walls of the water tank are covered using black cloth to diminish the reflection effect from the glass wall. Besides, a beam dump (Newport PL15), which is a device designed to absorb the energy of photons or other particles within an energetic beam, is installed near the back wall inside the glass tank to totally eliminate the effect of reflection. The transmission power is fixed at 50 mW during all the measurements except for the path loss measurements as a function of transmission power. Furthermore, to ensure that the scattered light is purely coming from water, a large enough blackboard was installed between the transmitter and receiver to block off any scattered light from the air. All the measurements were in a darkroom at a temperature of $\sim 20^\circ\text{C}$.

At the receiver end, a power meter (Newport 2936-C) and a photodetector (Newport 818-UV/DB) with wavelength response in the range of 200-1000 nm, a clear aperture of 10.3 mm, and calibration uncertainty without attenuator of $\pm 1\%$ @ 350 – 949 nm is utilized. Φ_{Tx} in Fig. 1 is the field-of-view (FOV) of the detector, which is 100° in our experiment. φ_{Tx} is the receiver azimuth angle that can be changed using a rotation stage.

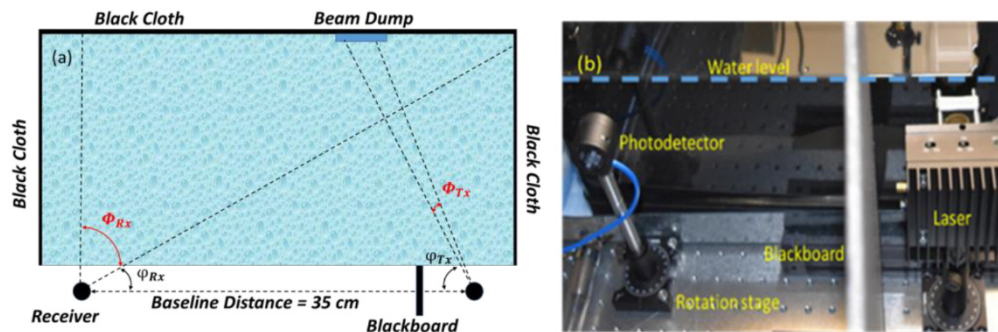


Fig. 1. Experimental setup: (a) block diagram indicating various parameters, and (b) an image of the setup.

In natural waters, the particle size range of interest is limited in the first approximation to roughly 0.01 to 1000 μm . This range is of interest to those researchers who are concerned with the optical properties of seawater and its influence on propagation of light in the sea [26]. In this investigation, the water turbidity is precisely controlled by adding commercial antacid (Maalox), which has suspension particles $\text{Al}(\text{OH})_3$ and $\text{Mg}(\text{OH})_2$ with the particle size in part of the above interval range, resulting in both Mie scattering (forward scattering) and Rayleigh scattering. In laboratory experiments, Maalox solution is known to present excellent scattering characteristics similar to real ocean particles [27,28]. Laux et al. experimentally validated the use of Maalox as scattering agent by measuring and comparing its volume scattering function (VSF) against two different measurements in a 3 m laboratory water tank in [27] which can be used as a baseline for determining the amount of Maalox concentration needed to emulate different ocean water types [13,29–31]. Volume (V in μL) of Maalox was calculated and added to the 23 liters of tap water in an orderly fashion based on [27] to produce four ocean waters, namely clear sea water, coastal water, harbor I water, and harbor II water. Before adding Maalox solution to simulate different water types, the tap water was

thoroughly characterized by measuring its attenuation coefficient and particle concentration. The attenuation coefficient was found to be 0.071 m^{-1} . Table 1 shows the desired attenuation coefficient, the added volume, and the resulting Maalox concentration (C in g/m^3) [28]. Each Maalox mixture was sufficiently stirred to obtain a uniform water channel before proceeding with the measurements.

Note that the value of attenuation coefficient of each water type including tap water slightly changes between geographic locations [32–34]. However, this variation is not that significant and may not influence the results of our study since the VSF of tap water is two to three orders of magnitude lower than that of ocean waters, such as clear ocean water, that is highly peaked in the near forward direction [28,35].

Table 1. Calculated Maalox amounts for simulating four different types of water.

Water Type	$c \text{ (m}^{-1}\text{)}$	$V \text{ (}\mu\text{L)}$	$C \text{ (g/m}^3\text{)}$
Clear sea water	0.151	70	0.3
Coastal water	0.398	183	0.7
Harbor I water	1.1	507	2
Harbor II water	2.19	1009	3.9

3. Results and discussion

Focusing on the baseline distance of $D = 35 \text{ cm}$, the received power (P_r), after the beam passing through the channel, was measured for several azimuth angles of both the transmitter (φ_{Tx}) and the receiver (φ_{Rx}) using the 375-nm laser under clear water (without Maalox), as shown in Fig. 2(a). In general, the received power increases with the decrease of azimuth angles, because of the higher chance for photons to be scattered into the FOV of the receiver.

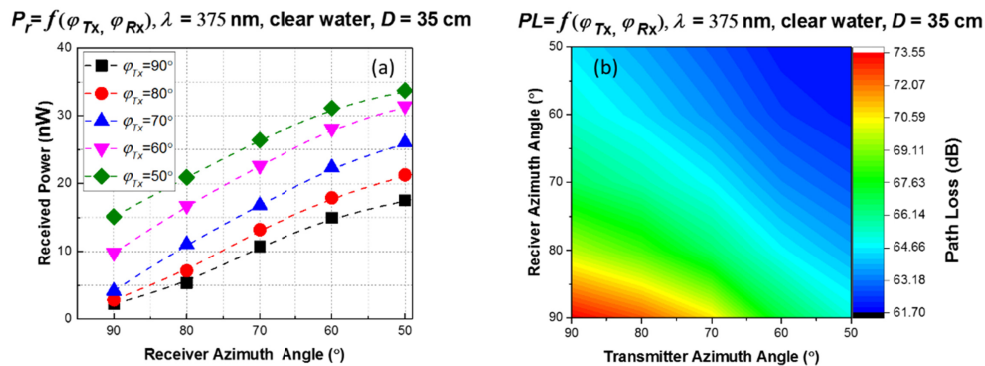


Fig. 2. (a) Received power and (b) Contour plot of path loss versus azimuth angles using 375-nm laser diode in clear water at a baseline distance of $D = 35 \text{ cm}$.

Figure 2(b) shows the contour plot of the calculated path loss (PL) based on the measured results in Fig. 2(a). The path loss was calculated and presented in logarithmic form according to the following formula [22]:

$$PL = 10 \times \log_{10} \left(\frac{P_t}{P_r} \right) \quad (1)$$

where PL is the logarithmic path loss (dB), P_t is the transmitted power, which is 50 mW. The highest path loss is 73.55 dB when both of φ_{Tx} and φ_{Rx} are 90°, while the lowest path loss is around 61.70 dB when both of φ_{Tx} and φ_{Rx} are 50°.

To demonstrate the significant advantage of the wavelength of 375-nm in NLOS communication, the path loss measurement was also conducted using a 50-mW, 405-nm laser

for comparison, which is a wavelength in the “transparent window” utilized in UWOC for LOS communications due to a low water absorption coefficient.

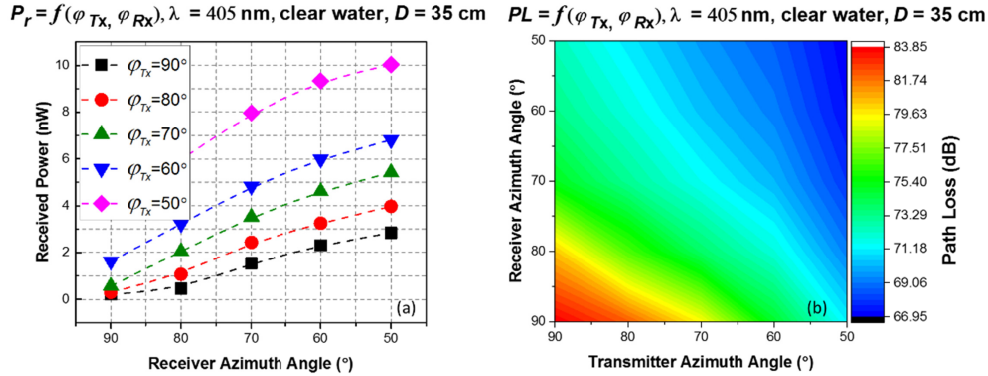


Fig. 3. (a) Received power and (b) Contour plot of path loss versus azimuth angles using 405-nm DPSS laser in clear water at a baseline distance of $D = 35$ cm.

Figure 3(a) shows the received power for all the combinations of transmitter and receiver azimuth angles using 405-nm laser. Compared with P_r & PL of the 375-nm laser in Fig. 2, it can be found that the received power for 405-nm laser is generally lower than that of 375 nm laser. For example, $P_r = 10$ nW when $\varphi_{Tx} = 50^\circ$, $\varphi_{Rx} = 50^\circ$, while the corresponding value for the 375-nm laser is 34 nW. This can be explained partly and qualitatively according to Rayleigh scattering principle [36]:

$$I \sim \frac{1}{\lambda^4} \quad (2)$$

Shorter wavelength has stronger scattering effect. Therefore, the wavelength of 375-nm has stronger scattering underwater, resulting in lower path loss in NLOS UWOC links. Hence, from the perspective of high SNR induced by high received power, wavelength of 375-nm is much more suitable to be utilized in short range NLOS UWOC communications. Figure 3(b) shows the contour plot of losses for 405-nm laser. Similar to the case of 375-nm laser, higher azimuth angles results in higher losses. Having established that the path loss performance for NLOS underwater link is superior when 375-nm wavelength is utilized, as compared to the measurement of 405-nm laser, the following measurements further focus on path loss studies based on the 375-nm laser.

Besides the azimuth angles, the received power and path loss will also be affected by the baseline distance D . It is expected that the received power increases when the baseline distance is shortened. This is not only due to the increase in overlap between the FOV of the photodetector and the laser beam but also resulted from a reduction in absorption loss. Here, we considered baseline distance, $D = \{35, 32.5, 30, 27.5, 25, 22.5\}$ cm while fixing the azimuth angles both of the transmitter and receiver at 90° in order to obtain the measurements for the extreme cases in NLOS communication. Figure 4 shows an increase in the received power of 37.8 nW or a corresponding reduction in path loss of 12.6 dB when the baseline distance was shortened from 35 cm to 22.5 cm. The linear regime gave a slope of $1.26 \text{ dB}\cdot\text{cm}^{-1}$. This value serves as a useful reference to estimate the baseline distance when the 375-nm laser is used for a NLOS communication link in clear water.

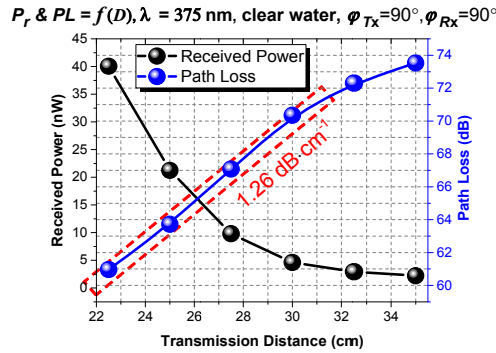


Fig. 4. Received power and path loss for 375-nm laser when propagating in clear water with a NLOS configuration at baseline distance $D = \{35, 32.5, 30, 27.5, 25, 22.5\}$ cm under extreme case of $\varphi_{Tx} = 90^\circ, \varphi_{Rx} = 90^\circ$.

The previous measurements were taken under clear water conditions. However, the particles in natural waters enhance scattering effect, which is a function of individual scattering cross-sections and concentration [26]. Thus, an environment rich in scattering centers is expected to reduce the NLOS path loss. We simulate different water types by adding a various amount of Maalox to clear water, as described in Table 1. Figure 5 (a) shows the received power and losses when fixing the azimuth angle of both transmitter and receiver at 90° with a baseline distance of 35 cm. As expected, harbor II water has lowest losses because of scattering enhanced by its highest water turbidity, followed by harbor I water, and coastal water, while the clear sea water exhibited the highest path losses. Such behaviors are attributed to the scattering effects, which compensate the optical absorption. Therefore, it is feasible to construct a few meters, even tens of meters NLOS UWOC communication link using a 375-nm laser in harbor II water condition by increasing the transmission power for further enhancing multiple scattering and propagation distance. Figure 5 (b) evidently shows the increase in laser beam divergence and scattering with increasing water turbidity in (i) clear sea water; (ii) coastal water; (iii) harbor I; (iv) harbor II.

$$P_r \text{ \& \; } PL = f(n), \lambda = 375 \text{ nm}, \varphi_{Tx} = 90^\circ, \varphi_{Rx} = 90^\circ, D = 30 \text{ cm}$$

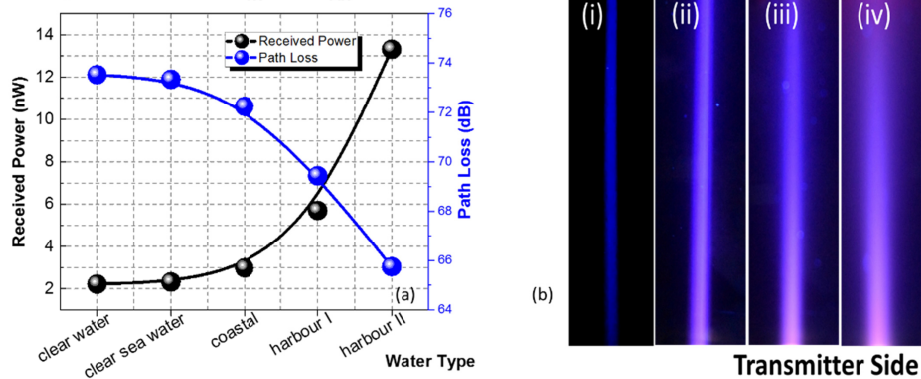


Fig. 5. (a) Received power and path loss for 375-nm laser in four types of water with a baseline distance of $D = 35$ cm. (b) Photos of beam divergence and scattering under different water turbidity: (i) clear sea water; (ii) coastal water; (iii) harbor I; (iv) harbor II.

4. Conclusions

We demonstrated that NLOS UWOC link can be significantly enhanced using a 375-nm laser. It holds promises for circumventing the problems of scintillation, deep-fade, complete signal blockage in LOS UWOC. Based on this link, we experimentally measured the effect of

geometries (azimuth angles, baseline distance), and water turbidity (clear sea water, coastal water, harbor I, harbor II water), and wavelength (375 nm and 405 nm) on path loss. This comprehensive path loss study is crucial for laying the foundation for future evaluation of communication data rate and received SNR performances. The experimental results suggest that path loss of such links are favorable for smaller azimuth angles, stronger water turbidity, and shorter transmission wavelength, as exemplified by the use of 375-nm wavelength. Our work highlighted the potential to establish a NLOS UWOC link over tens of meters by using 375 nm laser, even in turbid water media, including harbor waters.

Funding

King Abdulaziz City for Science and Technology (KACST) Grant KACST TIC R2-FP-008; King Abdullah University of Science and Technology (KAUST) BAS/1/1614-01-01, KCR/1/2081-01-01, GEN/1/6607-01-01, REP/1/2878-01-01.